

Preparation of TiO₂ Nanolayers via. Sol-Gel Method and Study the Optoelectronic Properties Assolar Cell applications

¹Khalid Haneen Abass, ²Mohammed Hadi Shinen and ³Ayad F. Alkaim

¹Department of Physics, College of Education for Pure Sciences,

²Department of Science, College of Basic Education,

³Department of Chemistry, College of Science for Women, University of Babylon, Hillah, Iraq

Abstract: The aim of this research is to prepare TiO₂ films on Indium Tin Oxid (ITO)-glass substrates with various nano-layers via. sol-gel method and study the properties that make these films suitable for solar cell application. Polycrystalline TiO₂ films are resulting from X-Ray Diffraction (XRD) examination with preferred orientation along (101) plane appear for the films with thickness more than 107 nm (3 layers) at $2\theta = 25.62^\circ$. Other peaks appear (211), (004) and (200) at $2\theta = 30.27, 35.49$ and 48.69 , respectively and the crystallite size ranged from 15-32 nm for the prepared films. The homogeneity of the films is appear from the scanning electron microscope in addition of smooth and free of pinholes. UV-Visible spectrophotometer use to recording the transmittance spectra in the range of 360-1000 nm. The energy gaps were determined by Touc Model and from the dispersion parameters which found good comparable to be 3.21 eV for the film thickness 155 nm (5 layers). The energy loss of electrons which travelling through surface and bulk of material also determined. Urbach energy is increase with the increasing of film thickness. Dispersion parameters (E_o , E_d) determined from Wemple and DiDomenco relationship.

Key words: Sol-gel, TiO₂ layers, dispersion parameters, single-oscillator model, surface, comparable

INTRODUCTION

Many purposes for preparing TiO₂ thin films or nanoparticles by sol-gel method; thin layers of (TiO₂) with a high photocatalytic activity and antibacterial properties for use as a self-cleaning transparent coatings for windows in outdoors applications (Haider *et al.*, 2017) biosensor (Cui *et al.*, 2018) by doping TiO₂ onto CNTs, among applications of CNTs that have optical property to its application in micro electronic and electro-opticindustry (Askari *et al.*, 2017) C, N co-doped TiO₂ noticeably increase in the visible-light-photocatalytic activity performance is ascertained mainly due to the improvement of electron-hole separation and charge carrier migration (Mohamed *et al.*, 2018) Titanium dioxide (TiO₂) is a cheap, non-toxic and one of the most efficient semi conductor photo catalysts for extensive environmental applications because of its strong oxidizing power, high photochemical corrosive resistance and cost effectiveness (Weast and Selby, 1967). Titanium dioxide occurs in nature as the well-known naturally occurring minerals (Rusu and Rusu, 2005) rutile with energy gap 3.05 eV, anatase with energy gap 3.26 eV (Carp *et al.*, 2004) and brookite with energy gap 2.98 eV

(Stankova *et al.*, 2009). This range of band gap of is suitable for a variety of applications, especially in solar cells (Yalcin and Yakuphanoglu, 2017; Chen *et al.*, 2017; Choe and Han, 2017; Murugakoothan *et al.*, 2014). Although, preparation is important in a sol-gel method, however, many researchers have been prepared titanium oxide in other methods such as; PLD (Aadim *et al.*, 2015) RF magnetron sputtering (Goto *et al.*, 2015) spin-coating (Hsieh *et al.*, 2010; Mothi *et al.*, 2014) e-Beam evaporation (Hossain *et al.*, 2015) liquid phase deposition (Begum *et al.*, 2008) spray pyrolysis (Patil *et al.*, 2014). Due to the special attention focused onthe monolayer to obtain the unique properties that are found in the monolayer, therefore, it is important to study these structures (Jappor, 2017). In this study, layers are prepared from TiO₂ via. sol-gel method and study the structural and optical properties for various layers for solar cell application.

MATERIALS AND METHODS

Methods of synthesis and preparation of thin film: The three components used in the preparation of the TiO₂ sol-gel films can be explained as follows Titanium

Isopropoxide (TIP) $\text{Ti} [\text{OCH}(\text{CH}_3)_2]_4$ whose purity is 98%, Acetic acid CH_3COOH whose purity is 99.5% and Ethanol $\text{CH}_3\text{CH}_2\text{OH}$ whose purity is 99.7-100%. All chemicals are as supplied by Aldrich chemicals Ltd. TIP is a metal alkoxide which has the general formula $\text{M} (\text{OR})_n$ where, M = Metal, R = Alkyl group and n is the valence of the metal atom. TiO_2 thin films are prepared by sol-gel spincoating method by using 50 mL of Ethanol and permitting to be mixed for 50 min an amount of 5 mL of acetic acid with a pipette into Ethanol and stir by using a magnetic stirrer it for 5 min and measure 6.3 mL of TIP is added by pipette to a beaker containing a mixture of glacial acetic acid and ethanol that have been mixed for 5 min. The mixture is continually stirred by using a magnetic stirrer addition for further 2 min after adding of the precursor. The effects of altering molar ratios of acid TIP on thickness and absorption properties of the films are investigated. The sols manufactured due to the method described above are immediately used to produce coating on the Indium Tin Oxid (ITO)-glass substrates. Thin films of TiO_2 are deposited by the method of spin coating by using a standard photoresist spinner. Glass plates coated with transparent conducting (ITO) are used as substrates, these have been thoroughly cleaned in Millipore water and neutral detergent for 10 min by using an ultrasonic bath and then propanol has been applied for further 10 min in the ultrasonic bath. The solution is placed into a convenient glass flask and is sealed well. This sealing should keep the solution from contaminated air. Finally the substrates have been rinsed by deionized water and then dried out with nitrogen gas. TiO_2 films are spin coated onto the cleaned (ITO) substrates with a spinning speed 2000 rpm. All samples in the furnace program are put at 550°C

RESULTS AND DISCUSSION

Structural analysis of films: The crystal structure of TiO_2 films that prepared via. sol-gel method at various layers on ITO substrates were investigated using X-Ray Diffraction (XRD). Figure 1 represents the XRD pattern to evaluate the crystallographic properties of TiO_2 film layers that deposited on ITO substrate. The XRD results show that the films with thickness 37, 72 nm (1, 2 layers, respectively) are amorphous and when the thickness increase lead to the polycrystalline films (107, 126, 155 nm (3-5 layers, respectively)). The TiO_2 polycrystalline films has an orientation peak along (101) plane at $2\theta = 25.62^\circ$ and the other peaks corresponding to the (211), (004) and (200) at $2\theta = 30.27^\circ$, 35.49° and 48.69° , respectively. The crystallite size (D) was estimated by scherrer formula (Krawitz, 2001).

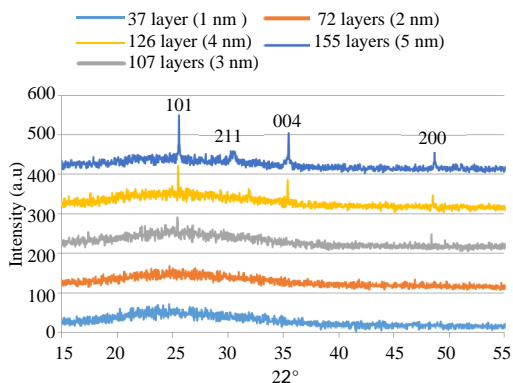


Fig. 1: XRD pattern of TiO_2 films with various layers

$$D = \frac{k\lambda}{\beta \cos \theta} \quad (1)$$

Where:

K = The Scherrer constant and equal 0.94

λ = The wavelength of X-ray (1.54060 \AA)

β = The Full Width at Half Maximum (FWHM) for the peaks and

θ = The Bragg diffraction angle

The crystallite size was calculated from Scherrer formula to be 15 nm (FWHM = 0.224) and increased with the increasing of film thickness to be 33 nm for the film with thickness 155 nm (FWHM = 0.454)

The morphological properties of TiO_2 films can determine from Scanning Electron Microscope (SEM). Figure 2 illustrates the homogeneity and continuous separate coating layers and also it can be seen the films are smooth and free of pinholes.

Optical properties: The optical properties of TiO_2 nanoparticle layers are determined from recording the absorbance and transmittance spectra via. UV-Visible spectro photometer (UV/1800/Shimadzu spectro photometer) in the wavelength range 360-1000 nm.

The transmittance spectra were presented in Fig. 3. From Fig. 3, it can be noticed the decrease of transmittance with the increasing of thickness (number of layers) for the TiO_2 nanoparticle films. The values of transmittance spectra are ranged from 60-80% approximately in the visible region, making these films suitable for solar cell applications. The optical energy gap (E_g) of nanostructure TiO_2 layers can be determined from the following relation (Abass, 2015):

$$(\alpha h\nu)^n = B(h\nu - E_g) \quad (2)$$

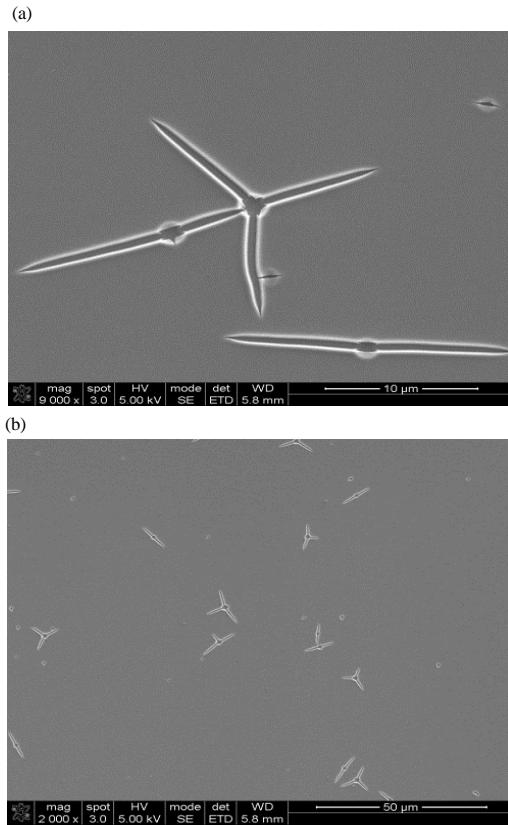


Fig. 2: SEM images of annealed TiO₂ film

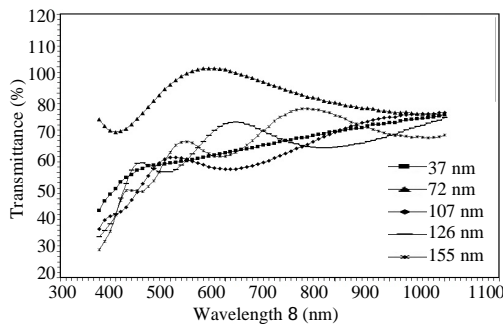


Fig. 3: Transmittance spectra of TiO₂ films for various thickness

Where:

$h\nu$ = The photon energy, B is a constant and
 n = The allowed transition type ($n = 2$ for direct transition, $n = 1/2$ for indirect transition)

To determine the optical energy gap, it can plot the $(\alpha h\nu)^2$ on the y-axis versus photon energy on the x-axis, the extrapolation that intercept with x-axis represent the value of energy gap (Abass and Latif, 2016) as shown in Fig. 4. The values of energy gap for TiO₂ films are

decreased with the increasing of number of layers from 3.3 eV for one layer (37 nm) to 3.21 eV for five layers (155 nm).

The complex dielectric constant is very important because provides information about electronic structure of the films. There Al part of dielectric constant (ϵ_r) describes the propagation characteristics while the imaginary part (ϵ_i) describes the rate of attenuation along the propagation direction were calculated using the formulas (Buet *et al.*, 1991):

$$\epsilon_r = n^2 - k^2 \quad (3)$$

$$\epsilon_i = 2nk \quad (4)$$

where, k is the extinction coefficient. The real and imaginary dielectric constants are decreased with the increasing the number of layers of TiO₂ films as shown in Fig. 5.

The Surface Energy Loss Function (SELF) and Volume Energy Loss Function (VELF) are represent the energy loss of electrons which travelling through surface and bulk of material, respectively which obtained from complex dielectric constant as the following formulas (Mahmoud, 1987; Park, 2012):

$$\text{SELF} = \frac{\epsilon_i}{(\epsilon_r + 1)^2 + \epsilon_i^2} \quad (5)$$

$$\text{VELF} = \frac{\epsilon_i}{\epsilon_r^2 + \epsilon_i^2} \quad (6)$$

The SELF and VELF versus photon energy are presented in Fig. 6 and 7, respectively. From the Fig. 6 and 7, the SELF and VELF are decreased with the increasing of number of layers (thickness) leads to less loss of electron energy with the increasing of thickness. Also, the values of surface energy loss are less than the volume energy loss, this result is agreement with the researcher Wug-Dong (Park, 2012).

The tail of the absorption edge is exponential, indicating the presence of localized states in the energy band gap. The amount of tailing represent the Urbach Energy (E_U) and given by the following formula (Urbach, 1953):

$$\alpha = \alpha_0 \exp(h\nu/E_U) \quad (7)$$

Where:

α_0 = The α constant and
 $h\nu$ = The photon energy

To determine the value of Urbach energy, it can plotting $\ln \alpha$ as a function of photon energy as shown in the Fig. 8

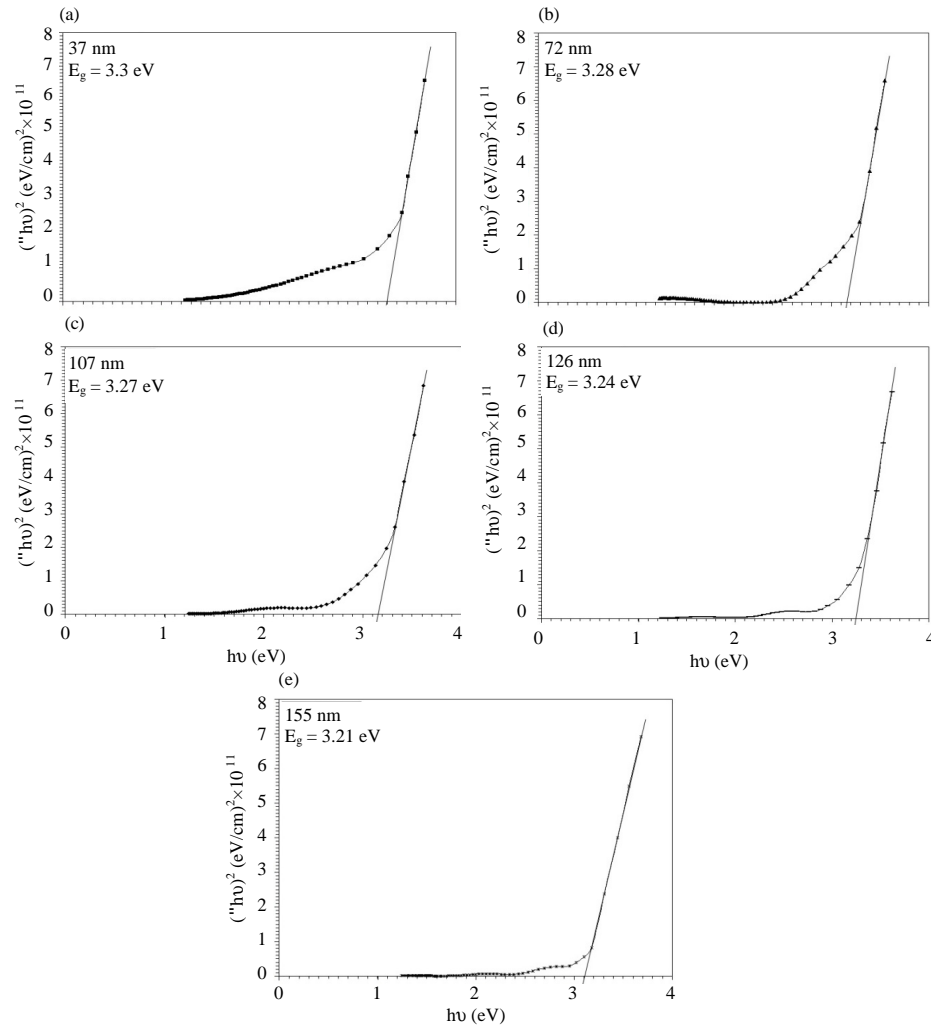


Fig. 4: Plot of $(\alpha h\nu)^2$ versus $h\nu$ for TiO_2 films; a) 37 nm; b) 72 nm; c) 107 nm; d) 126 nm and e) 155 nm

The values of E_0 are increase with the increasing of number of layers for the prepared TiO_2 films which listed in the Table 1, refer to the broadening of tails inside the energy gap

The dispersion energy is an important for optical materials because it is a significant factor in optical communication and in designing devices for spectral dispersion. The dispersion of refractive index of TiO_2 nanoparticle layers are determined using the single oscillator that expressed by Wemple and DiDomenico relationship as following (Wemple and DiDomenico Jr., 1969):

$$n^2 - 1 = \frac{E_d E_0}{E^2 E^2} \quad (8)$$

Where:

E_0 = The single oscillator energy of the electronic transitions

E_d = The dispersion energy, $E = h\nu$ is the photon energy

n = The refractive index

Figure 9 represent the plot of $(n^2 - 1)^{-1}$ versus $(h\nu)^2$ which used to determine the values of E_0 and E_d from the slope $(E_0 E_d)^{-1}$ and intercept (E_0/E_d) (Mishjil *et al.*, 2016).

From Wemple and DiDomenico relationship can determine the value of energy gap from a close approximation $E_0 \approx 2E_g$ (Wemple and DiDomenico, 1971). The values of zero frequency refractive index (n_0) can be determined from the Eq. 8 and the zero frequency dielectric constant can be determined from $\epsilon_0 = n_0^2$ (Guler and Gasanly, 2007). The values of ϵ_0 and n_0 are decreased with the increasing of number of layers as listed in Table 1.

The moments of the optical spectra (M_1 and M_3) of TiO_2 films were calculated from the following equation (Abass and Latif, 2016; Yakuphanoglu *et al.*, 2004):

$$E_0^2 = \frac{M_1}{M_3} \quad (9)$$

The values of M_1 and M_3 are decreased with the increasing of number of layers as shown in Table 1.

$$E_d^2 = \frac{M_{-1}^3}{M_3} \quad (10)$$

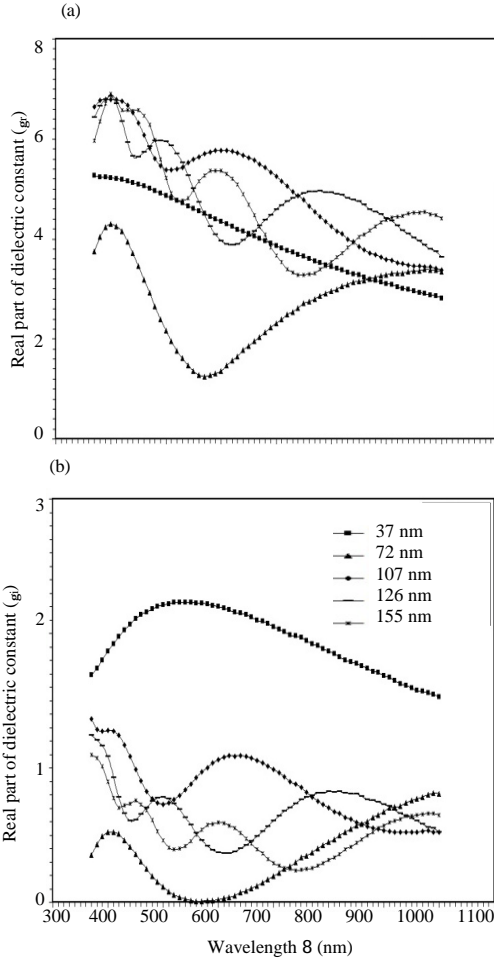


Fig. 5: Dielectric constant of TiO_2 film for various thickness; a) Real and b) Imaginary parts

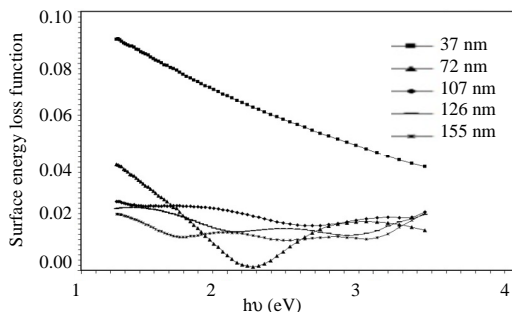


Fig. 6: Surface energy loss function of TiO_2 film for various thickness

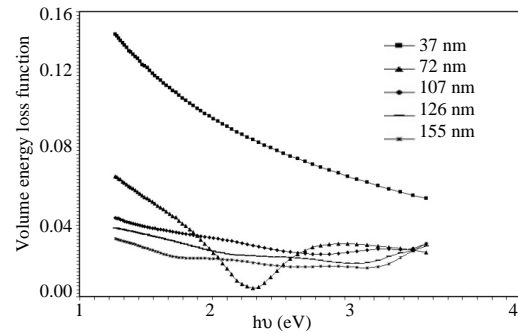


Fig. 7: Volume energy loss function of TiO_2 film for various thickness

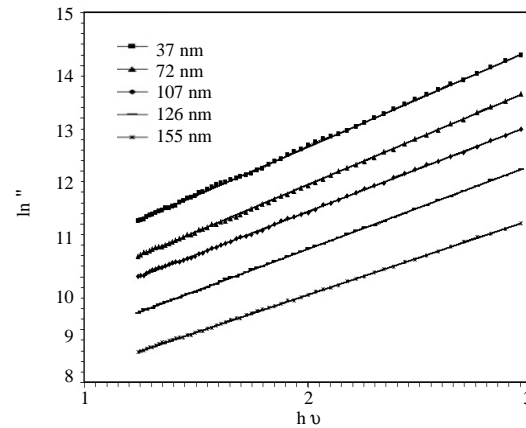


Fig. 8: Plot of $\ln \alpha$ versus $h\nu$ of TiO_2 films with various thickness

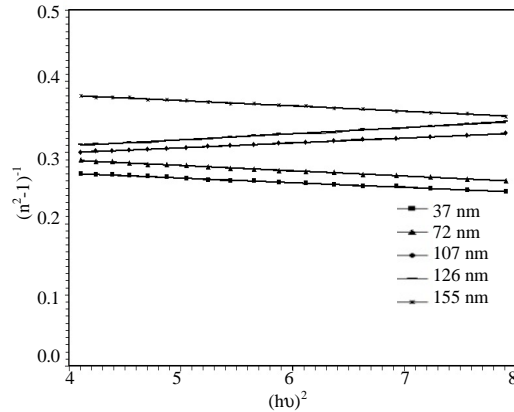


Fig. 9: Plot of $(n^2-1)^{-1}$ versus $(h\nu)^2$ of TiO_2 films with various thickness

Table 1: The Urbach energy and dispersion parameters of nanostructure TiO₂ films

TiO ₂ thickness (nm)	E _U (meV)	E _d (eV)	E _g (eV)	E _g (eV)	n(o)	ε _o	M ₁ (eV ⁻²)	M ₃ (eV ⁻²)×10 ²
37	549	24.40	6.83	3.41	2.13	4.57	3.571	7.653
72	568	23.21	6.73	3.36	2.11	4.44	3.448	7.610
107	609	22.85	6.62	3.34	2.10	4.38	3.440	7.580
126	657	19.29	6.56	3.28	1.99	3.94	2.940	6.834
155	699	17.97	6.46	3.23	1.95	3.78	2.780	6.636

CONCLUSION

In this research, nano-layers of TiO₂ were prepared by sol-gel method onto ITO substrates and annealed at 550°C. Structural and optical properties are investigated to use these films in solar cell application. The nanostructure TiO₂ films have been characterized using XRD which reveal the preferred orientation along (101) plane and other peaks that refer to the TiO₂ anatase phase. Crystallite size ranged from 15-32 nm that estimated from Scherrer formula. The SEM analysis showed the films are smooth, homogeneous and free of pinholes. From recording the transmittance spectra, the optical parameters are determined and the energy gap that calculated via. Touc model and from dispersion parameters. The energy gap was decreased with the increasing of film thickness while the Urbach energy increased. The energy loss of electrons which travelling through surface and bulk of material are decreased with the increasing of thickness. Dispersion parameters (E_g, E_o) are decreased with the increasing of film thickness and the moments of the optical spectra (M₁ and M₃) also decreased.

REFERENCES

- Aadim, K.A., K.H. Abass and Q.M. Hadi, 2015. Effect of annealing temperature on the optical properties of TiO₂ thin films prepared by pulse laser deposition. *Intl. Lett. Chem. Phys. Astron.*, 56: 63-70.
- Abass, K.H. and D.M.A. Latif, 2016. The Urbach energy and dispersion parameters dependence of substrate temperature of CdO thin films prepared by chemical Spray Pyrolysis. *Intl. J. Chem. Technol. Res.*, 9: 332-338.
- Abass, K.H., 2015. Fe₂O₃ thin films prepared by spray Pyrolysis technique and study the annealing on its optical properties. *Intl. Lett. Chem. Phys. Astron.*, 45: 24-31.
- Askari, M.B., Z.T. Banizi, M. Seifi, S.B. Dehaghi and P. Veisi, 2017. Synthesis of TiO₂ nanoparticles and decorated Multi-Wall Carbon Nanotube (MWCNT) with anatase TiO₂ nanoparticles and study of optical properties and structural characterization of TiO₂/MWCNT Nanocomposite. *Intl. J. Light Electron. Opt.*, 149: 447-454.
- Begum, N.S., H.F. Ahmed and K.R. Gunashekar, 2008. Effects of Ni doping on photocatalytic activity of TiO₂ thin films prepared by liquid phase deposition technique. *Bull. Mater. Sci.*, 31: 747-751.
- Buet, F., J. Olivier-Fourcade, Y. Bensimon and P. Belougne, 1991. Complex impedance study of Chalcogenide glasses. *Solid State Commun.*, 77: 29-32.
- Carp, O., C.L. Huisman and A. Reller, 2004. Photoinduced reactivity of titanium dioxide. *Prog. Solid State Chem.*, 32: 33-177.
- Chen, B.C., R. Umamaheswari, C. Su, V. Mani and Y.F. Lin *et al.*, 2017. Fabrication of flexible and efficient dye sensitized solar cells using modified TiO₂ electrode at low-temperature annealing process. *J. Nanoelectron. Optoelectron.*, 12: 872-879.
- Choe, G. and Y.S. Han, 2017. Silanization of TiO₂ surface and its influences on the photovoltaic properties of dye-sensitized solar cells. *J. Nanoelectron. Optoelectron.*, 12: 602-606.
- Cui, H.F., W.W. Wu, M.M. Li, X. Songa and Y. Lv *et al.*, 2018. A highly stable acetylcholinesterase biosensor based on chitosan-TiO₂-graphene nanocomposites for detection of organophosphate pesticides. *Biosens. Bioelectron.*, 99: 223-229.
- Goto, S., Y. Adachi, K. Matsuda and M. Nose, 2015. Crystal structure and optical properties of TiO₂ thin films prepared by reactive RF Magnetron Sputtering. *Arch. Metall. Mater.*, 60: 965-967.
- Guler, I. and N.M. Gasanly, 2007. Optical properties of TiGaSeS layered single crystals. *J. Korean Phys. Soc.*, 51: 2031-2035.
- Haider, A.J., R.H. AL-Anbari, G.R. Kadhim and C.T. Salame, 2017. Exploring potential Environmental applications of TiO₂ Nanoparticles. *Energy Procedia*, 119: 332-345.
- Hossain, F., A. Al-Asad, O. Faruk and A.I. Nahid, 2015. Analysis the electrical properties of CO, TiO₂ and CO/TiO₂ multilayer thin films of different thickness deposited by E-beam technique. *Am. J. Eng. Res.*, 4: 48-53.
- Hsieh, L.L., C.Y. Chang, H.L. Shyu, C.A. Tsou and H.H. Lo, 2010. The inhibition effect of TiO₂/Ag thin film on *Acinetobacter baumannii*. *Adv. Mater. Res.*, 123: 272-275.
- Jappor, H.R., 2017. Electronic and structural properties of gas adsorbed graphene-silicene hybrid as a gas sensor. *J. Nanoelectron. Optoelectron.*, 12: 742-747.
- Krawitz, A.D., 2001. Introduction to Diffraction in Materials Science and Engineering. John Wiley and Sons, Hoboken, New Jersey, USA., ISBN:9780471247241, Pages: 424.
- Mahmoud, S., 1987. Optical properties of tin in the 2.5 to 40 im region. *J. Mater. Sci.*, 22: 251-256.

- Mishjil, K.A., S.S. Chiad, K.H. Abass and N.F. Habubi, 2016. Effect of Al doping on structural and optical parameters of ZnO thin films. *Mater. Focus*, 5: 471-475.
- Mohamed, M.A., J. Jaafar, M.F.M. Zain, L.J. Minggu and M.B. Kassim *et al.*, 2018. Concurrent growth, structural and Photocatalytic properties of hybridized C, N co-doped TiO₂ mixed phase over gC₃N₄ Nanostructured. *Scr. Mater.*, 142: 143-147.
- Mothi, K.M., G. Soumya and S. Sugunan, 2014. Effect of calcination temperature on surface morphology and photocatalytic activity in TiO₂ thin film prepared by spin coating technique. *Bull. Chem. React. Eng. Catal.*, 9: 175-181.
- Murugakoothan, P., S. Ananth, P. Vivek and T. Arumanayagam, 2014. Natural dye extracts of areca Catechu nut as dye sensitizer for Titanium Dioxide based dye sensitized solar cells. *J. Nano Electron. Phys.*, 6: 1003-1-1003-4.
- Park, W.D., 2012. Optical constants and dispersion parameters of CDS thin film prepared by chemical bath deposition. *Trans. Electr. Electron. Mater.*, 13: 196-199.
- Patil, L.A., D.N. Suryawanshi, I.G. Pathan and D.G. Patil, 2014. Nanocrystalline Pt-doped TiO₂ thin films prepared by spray Pyrolysis for Hydrogen gas detection. *Bull. Mater. Sci.*, 37: 425-432.
- Rusu, R. and G. Rusu, 2005. On the electrical of TiO₂ thin film. *J. Optoelectron. Adv. Mater.*, 7: 234-238.
- Stankova, N.E., I.G. Dimitrov, T.R. Stoyanchoy, P.A. Atanasov and D. Kovacheva, 2009. Structure and optical anisotropy of pulsed-laser deposited TiO₂ films for optical applications. *Appl. Surf. Sci.*, 255: 5275-5279.
- Urbach, F., 1953. The long-wavelength edge of photographic sensitivity and of the electronic absorption of solids. *Phys. Rev.*, 92: 1324-1326.
- Weast, R.C. and S.M. Selby, 1967. *Handbook Chemistry and Physics*. 3rd Edn., CRC Press, Boca Raton, Florida, USA., Pages: 1245.
- Wemple, S.H. and M. DiDomenico Jr., 1969. Optical dispersion and the structure of solids. *Phys. Rev. Lett.*, 23: 1156-1160.
- Wemple, S.H. and M. Didomenico, 1971. Behavior of the electronic dielectric constant in covalent and ionic materials. *Phys. Rev. B*, 3: 1338-1351.
- Yakuphanoglu, F., A. Cukurovali and I. Yilmaz, 2004. Determination and analysis of the dispersive optical constants of some organic thin films. *Phys. B: Condensed Matter*, 351: 53-58.
- Yalcin, M. and F. Yakuphanoglu, 2017. Graphene-TiO₂ Nanocomposite Photoanode based on Quantum dot solar cells. *J. Nanoelectron. Optoelectron.*, 12: 254-259.